

RESEARCH PAPER

## Biosynthesis of Manganese Nanoparticle by using Milk Thistle (*Silybum Marianum*) Seeds Extract and Role in Carcinoma Cell Line

Linda Fawzi Abdul-Sattar <sup>1\*</sup>, Suhaib Raad Qasim <sup>2</sup>, Ahmed Thamer Wali <sup>1</sup>

<sup>1</sup> Industrial Applications and Material Technology Research Center, Scientific Research Commission, Ministry of Higher Education and Scientific Research, Baghdad, Iraq

<sup>2</sup> Medical Laboratory Technique Department, College Of Health and Medical Techniques, Ministry of Higher Education and Scientific Research, Al-Bayan University, Baghdad, Iraq

### ARTICLE INFO

#### Article History:

Received 08 September 2024

Accepted 27 December 2024

Published 01 January 2025

#### Keywords:

Biosynthesis

Carcinoma cell line

Manganese nanoparticles

*Silybum marianum*

### ABSTRACT

*Silybum marianum*, commonly known as milk thistle, is a botanical species that has been utilized in various traditional medicinal practices and is regarded as a promising ancient herb. The objective of the current investigation was to synthesize and characterize MnO nanoparticles utilizing milk thistle seed extract. The production of MnO<sub>2</sub> nanoparticles was accomplished through the combination of manganese acetate and a heated aqueous extract derived from dry milk thistle seeds. The MnO nanoparticles that were produced underwent characterization through various analytical techniques including UV-Visible spectroscopy, Fourier-transform infrared spectroscopy (FT-IR), X-ray diffraction (XRD), Energy-dispersive X-ray analysis (EDS), and Field emission scanning electron microscopy (FESEM) analysis. According to the findings of the investigations mentioned above, the produced MnO nanoparticles are spherical and 55 nm in size. The present study aimed to investigate the potential anticancer properties of Mn NPs and milk thistle seed extract against human breast cancer cells (MDA-MB-468). The half-maximal inhibitory concentrations (IC<sub>50</sub>) were determined to be 32.4 μg/mL after 48 hours of incubation. The Mn NP nanoparticles that have been synthesized exhibit noteworthy anti-cancer properties. The present study introduces a new environmentally sustainable approach for the synthesis of nanomaterials that possess enhanced or additional therapeutic properties originating from herbal sources. The biocompatibility and non-toxic characteristics exhibited by Mn NPs make them a suitable choice for employment in the field of biomedical applications. Despite this, it has been observed that Mn nanoparticles exhibit cytotoxic properties against cancerous cells, rendering them particularly advantageous for employment in the fields of cancer diagnosis and treatment.

#### How to cite this article

Abdul-Sattar L., Qasim S., Wali A. Biosynthesis of Manganese Nanoparticle by using Milk Thistle (*Silybum Marianum*) Seeds Extract and Role in Carcinoma Cell Line. J Nanostruct, 2025; 15(1):387-396. DOI: 10.22052/JNS.2025.01.036

### INTRODUCTION

Currently, nanotechnology is a developing branch of medical research that involves the study of intermediate structures between micromaterials and atomic structures. According to [1], this research is concentrated on improving physical

characteristics including surface area and volume ratio. The fact that herbal plants have a variety of medical qualities has made it easier to use their extracts in the creation of innovative medications [2]. The utilization of biological approaches,

\* Corresponding Author Email: [lindafawzi2015@gmail.com](mailto:lindafawzi2015@gmail.com)



This work is licensed under the Creative Commons Attribution 4.0 International License.

To view a copy of this license, visit <http://creativecommons.org/licenses/by/4.0/>.

particularly those derived from plants, presents a viable alternative to conventional methodologies for synthesizing nanoparticles, [3].

Plants contain various phytochemical ingredients such as alkaloids, polyphenols, flavonoids, and terpenoids, which can facilitate reducing of metal ions and lead to the formation of metal nanoparticles [4]. Furthermore, it has been demonstrated that biogenic plant Phyto-molecules possess the ability to enhance their fundamental characteristics, including antibacterial, antioxidant, and anticancer properties [5]. *Silybum marianum* had the general names *Cardus marianus* and milk thistle. Plant species was a biennial or annual plant of the Asteraceae family. This fully typical thistle had been purple to red flowers. Originally it was now found in the world [6]. The plant was cultured all over the world for the therapeutic potential of its seeds. The essential active compound in the plant seeds was a flavonoid known as silymarin, which was broadly used in redeveloping damaged hepatic tissues. Breast cancers r considered one of the most common malignancies that affect women [7]. The purpose of the experimental studies is to use seeds of medicinal plants (milk thistle) as a reducing agent for green synthesis of Mn nanoparticles with high stability which is used against breast cancer cell lines.

## MATERIALS AND METHODS

### Data Collection and Analysis

Manganese acetate  $[(\text{CH}_3\text{COO})_2 \text{Mn}_6\text{H}_2\text{O}]$  was bought from Sigma-Aldrich company (USA). Fresh seeds were collected from the plants garden of Baghdad University in March (2022), The plant name has been checked with <https://www.theplantlist.org>. and was earlier recognized by the National Herbarium of Iraq. Seeds are thoroughly washed twice with distilled water and air-dried for 14 days then, grind by a commercial grinder and stored in glass bottles for use.

### Preparation of the Plant Extract

A quantity of eight grams of dried seed powder was subjected to boiling for a duration of five minutes within an Erlenmeyer flask containing 200 mL of deionized water. The aqueous extract of the seed was subjected to cooling and filtration using What man paper No. 1. The mixture underwent a cooling process and was subsequently subjected to centrifugation at a rate of 3500 revolutions per minute for a duration of 15 minutes. The resulting

liquid portion was gathered into a container and subsequently preserved at a temperature of 5°C.

### Green Synthesis of Manganese Nanoparticles (Mn-NPs)

In the process of synthesizing manganese dioxide nanoparticles through a green approach, a solution containing 20 mL of 0.01 mM manganese acetate  $[(\text{CH}_3\text{COO})_2 \text{Mn}_6\text{H}_2\text{O}]$  and an aqueous solution with a pH of 8 were combined with 180 mL of seed extract (with an extract ratio of 90%). The mixture was stirred for 60 minutes at room temperature. In this stage, a solution was supplemented with 20 mL of turmeric, which is known to contain bioactive curcumin.

Patra [8] recently reported on the employment of curcumin extract as a stabilizing agent for MnO nanoparticles. Curcumin was synthesized through a process involving the addition of 16 g of powdered turmeric to a flask containing 400 mL of ethanol. The mixture was boiled for 5 minutes, allowed to cool, and then curcumin was added. The resulting mixture was subjected to centrifugation at 3500 rpm for 15 minutes. The transparent liquid was preserved at a temperature of 4 °C. The solution was subjected to centrifugation at a rate of 3000 revolutions per minute for a duration of 20 minutes to affect the separation of the nanomaterial from the reaction mixture. The resulting precipitate was subjected to multiple washes using deionized water and ethanol, after which it was suspended in 7 milliliters of deionized water. The precipitate was subsequently collected and subjected to drying in an oven at a temperature of 40°C. Finally, the NPs synthesized via green synthesis were stored in a glass bottle.

### Characterization of Synthesized Manganese Nanoparticles

The biosynthesis of MnNPs was first assessed through color alteration and validated by tracking the UV-vis absorption band via a double beam UV-visible spectrophotometer Model LT-2802, operating within the 300-800 nm wavelength range with 5 nm increments. X-ray diffraction is a technique used to analyze the atomic and molecular structure of materials by measuring the diffraction (XRD) measurement of seeds extract was done using a powder XRD diffractometer instrument (XRD – 6000 Shimadus, Japan) with  $\text{CuK } \alpha$  ( $=1.54 \text{ \AA}$ ) radiation. X-ray diffraction research used a glass plate dipped in a solution to make a manganese

nanoparticle. X-ray diffraction (XRD) analysis was conducted on seed extract using a powder X-ray diffractometer instrument (XRD-6000 Shimadus, Japan) within a  $2\theta$  angle range of  $10^\circ$  to  $80^\circ$ . Furthermore, a layer of manganese nanoparticles was generated through the immersion of a glass plate in a solution, followed by subsequent X-ray diffraction analyses. The sizing of the crystalline nanoparticle of manganese was conducted through an analysis of the X-ray diffraction peak widths. The characterization of functional groups linked to biomolecules was conducted through the utilization of Fourier Transform Infrared Spectroscopy (FT-IR) Tracer 100. The resolution of the instrument was set at  $4\text{ cm}^{-1}$  in ATR mode, and the range of analysis was between  $450 - 4000\text{ cm}^{-1}$ . The elemental composition was determined through the utilization of the Energy Dispersive X-ray Spectroscopy technique, specifically employing the EDX-6000 model. The investigation of the sample's surface morphology was conducted through the utilization of Field Emission Scanning Electron Microscopy (FE-SEM), which was performed using the Carl Zeiss SUPRA 40 VP instrument located in Oberkochen, Germany. The elemental composition was analyzed using the Energy Dispersive X-ray Spectroscopy of model EDX -6000.

#### Cell line: MDA-MB-468

Cailleau [9] acquired the MDA-MB-468 cell line from a 51-year-old woman with breast cancer, and it has since been used frequently in scientific research. The MDA-MB-468 cell line was derived from a pleural effusion of mammary glands and breast tissues and has been widely employed as a valuable tool for investigating the mechanisms underlying metastasis, migration, and proliferation in breast cancer.

#### Cytotoxicity Assay

Based on our previous work [10], we used the MTT assay to find out the risk that the Mn nanoparticles were for breast cancer cells (MDA-MB-468). Mn NP was dissolved at  $4800\text{ }\mu\text{g/ml}$  in a PBS solution with 0.5% DMSO, which was also used to make the necessary serial dilutions. First,  $(1 \times 10^4)$  cells/well were put into each well of a 96-well growth plate and left there overnight [11]. The contents of the wells were then changed to  $75\text{ }\mu\text{g/ml}$  of RPMI complete medium, which has 10% FBS and 1% penicillin/streptomycin. The cells

were treated with different amounts of Mn NP (12,5, 25, 50, 100, 200, and 400)  $\mu\text{g/ml}$  and free SLNs. The treated plates were put in an incubator at  $37^\circ\text{C}$  and 5%  $\text{CO}_2$  for 24 hours. After that, 100  $\mu\text{l}$  of MTT reagent (3-(4,5-dimethylthiazol-2-yl)-2,5-diphenyltetrazolium bromide, dissolved in RPMI at 0.5 mg/ml, was added to each well and left to sit for 4 hours at  $37^\circ\text{C}$  and 5%  $\text{CO}_2$ . Finally, 100  $\mu\text{l}$  /well of DMSO (Dimethyl Sulphoxide) was added to dissolve the purple-colored crystals of formazan that had formed. The absorbance (A) has been measured by an ELISA reader at 570 nm. At different concentrations, cell viabilities have been calculated by using the following equation. Cell viability =  $(A_{\text{sample}} / A_{\text{control}}) \times 100$ . The control group consisted of up of six wells/plates that had a PBS solution with 0.5% DMSO (25  $\mu\text{l}$ ) and RPMI (75  $\mu\text{l}$ ) [12]. Al-Shammari [13] used the following method to determine how much cell growth had been stopped (cytotoxicity).

$$\text{Cytotoxicity \%} = (\text{OD}_{\text{Control}} - \text{OD}_{\text{sample}}) / \text{OD}_{\text{Control}} \times 100$$

OSD control is the mean optical density of untreated wells,

$\text{OD}_{\text{sample}}$  is the optical density of treated wells.

#### Statistical Analysis

Results have been shown by the mean value and standard deviation. The software CalcuSyn, specifically the free version created by BIOSOFT in the United Kingdom, was used to determine the samples' IC50s. The study conducted by Mohammed [14] who employed One-way ANOVA using SPSS software version 22 in the United States, along with the least significant difference test (L.S.D) at a significance level of 5%. The purpose of this statistical analysis was to compare the anticancer activities of Mn-NPs on a breast cancer cell line.

## RESULTS AND DISCUSSION

#### Visual Observation

By the naked eye, changing of color from pale green to reddish yellow can be easily seen and confirmed synthesized of Mn nanoparticle (Fig. 1).

#### UV spectra analysis

The presence of an absorption edge at 360 nm is regarded as a strong indication of the beginning of Mn NP formation, which ranges within the 350-

500 nm designated for MnO<sub>2</sub> nanoparticles (Fig. 2).

#### Fourier Transform Infrared Spectroscopic Studies

The FT-IR range of manganese nanoparticles was represented in Fig. 3. FT-IR spectroscopy represents great sensitivity, specifically in detecting organic and inorganic content.

#### X-Ray Diffraction (XRD) Spectroscopic Studies

XRD spectrum has been used to examine Mn NPs that are synthesized by plant extract as shown in (Fig. 4). The diffraction pattern of synthesized

Mn NPs consists of sharp peaks at 19.5°, 20.7°, and 21.8° indicating polycrystalline type. Additionally, some less intense peaks were observed at 24°, 25.8°, 27° and 29.8°). The size of the particle could be calculated by using the Debye Scherrer equation (Eq. 1).

$$D = \lambda K / \beta \cos \theta$$

D is the mean of the particle size, the wavelength of the X-ray used is  $\lambda$  and  $\theta$  means the Bragg angle,  $\beta$  is the extensiveness of the pure deflection profile in radians on 2 $\theta$  scale and k is the constant



Fig. 1. Synthesis of Manganese nanoparticles from milk thistle seeds extract. A Milk thistle seeds extract. B. Manganese acetate. C. After the addition of manganese acetate.

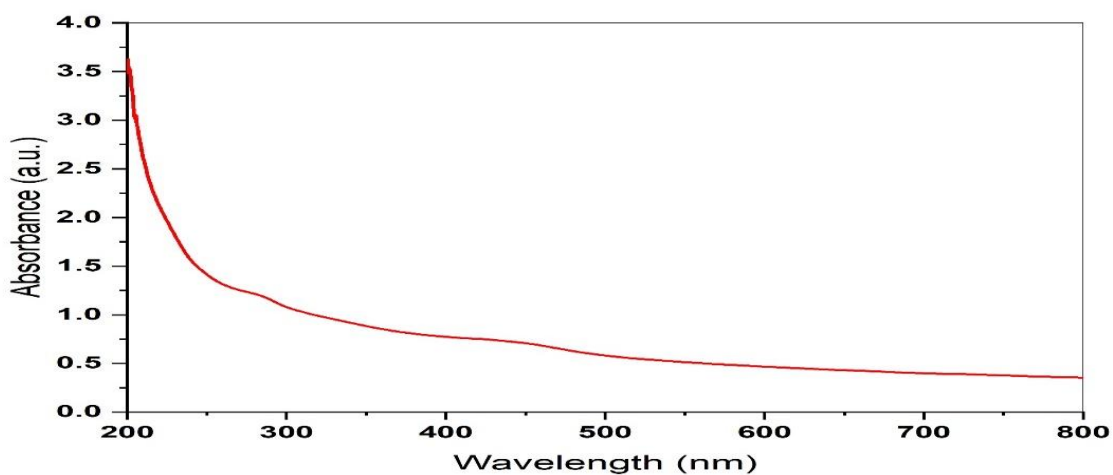


Fig. 2. UV-Vis spectra analysis of biosynthesized manganese nanoparticles by using milk thistle seed extract.

number. The results of the calculations indicate that the average particle size measures 55 nm and that the synthesis of MnNPs using milk thistle seed extract was successful.

*Field emission scanning electron microscopy (FE-SEM)*

The result of FESEM analysis represents the surface morphology and microstructure of MnO<sub>2</sub> nanoparticles (Fig. 5).

*Energy-dispersive X-ray analysis (EDX)*

EDX spectrum shows the existence of an energy absorption band at 6keV and was engaged to estimate the quantitative elemental structure which is the characteristic band of Manganese (Mn) thus; it confirmed the presence of elemental Mn. Manganese and Oxygen major peaks were detected in EDX spectra (Fig. 6) which return

to the elemental composition of the NPs and confirmed the presence of Mn and O with weight percentages of 11.5 and 88.5 respectively.

*Cytotoxicity assay*

The present study employed the MTT assay to investigate the cytotoxic efficacy of biosynthesized MnNPs against the MDA-MB-468 cell line. Various concentrations of Mn nanoparticles (12.5 µg/mL, 25 µg/mL, 50 µg/mL, 100 µg/mL, 200 µg/mL, 400 µg/mL) were prepared and administered to both cancerous and non-cancerous cells. The findings of the current investigation demonstrate the impact of Mn NP on both breast cancer cell lines and normal cells, as presented in Tables 1 and 2. Following a 48-hour incubation period, the findings indicated a noteworthy impact on MDA-MB-468 cells at concentrations of 50, 100, 200, and 400 µg/ml when compared to the control group.

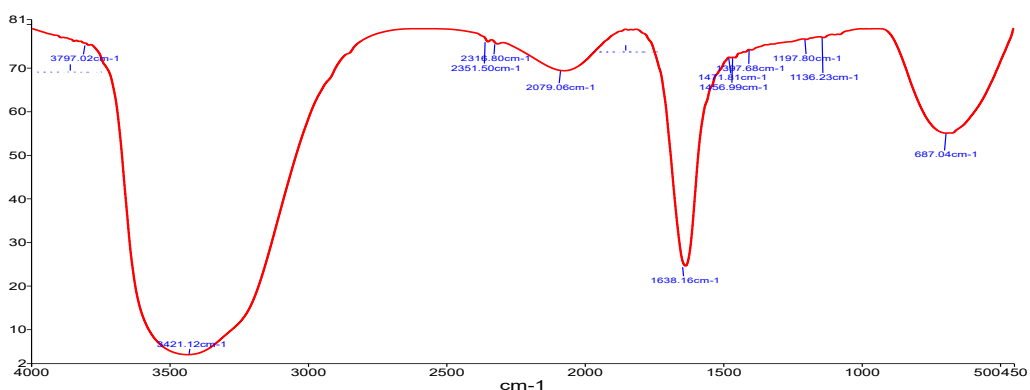


Fig. 3. FT-IR spectrum of biosynthesis manganese nanoparticles using milk thistle seeds extract.

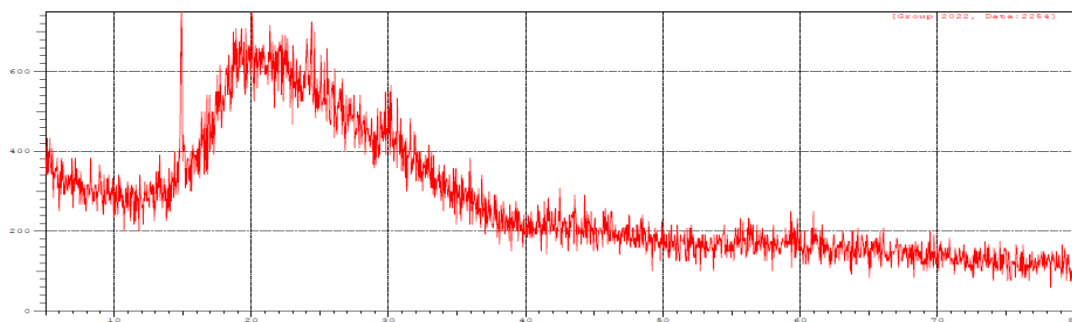


Fig. 4. X-ray diffraction pattern of biosynthesized manganese nanoparticle by using milk thistle seeds extract.

The percentages of cell growth inhibition were 32.8%, 101.8%, 107.1%, and 105.3%, respectively ( $p < 0.05$ ), an exception to the concentration of 12.5  $\mu\text{g/ml}$  ( $p > 0.05$ ). The growth inhibition percentage of the MDA-MB-468 cell line exhibits an increase in response to the escalating concentration of Mn NP. In general, the findings indicate that the growth inhibitory impact of Mn NP on the cell line was most pronounced at a concentration of 200  $\mu\text{g/ml}$ , corresponding to a value of 107.1%. This effect was found to be statistically significant when compared to the control group after 48 hours of incubation ( $p < 0.05$ ). Dose-dependent inhibitory

effects were observed on the proliferation of MDA-MB-468 cells from 50 to 200  $\mu\text{g/ml}$ , with a slight reduction in cell inhibitory observed after 400  $\mu\text{g/ml}$ . Table 2 displays the results of an MTT assay performed after 48 hours of incubation with various concentrations of Mn NP including (12.5, 25, 50, 100, 200, and 400)  $\mu\text{g/ml}$  on normal fibroblast cells, which revealed that Mn NP was able to inhibit fibroblast cells. After 48 hours of treatment, at concentrations of 100  $\mu\text{g/ml}$ , cytotoxic effects were greatest against fibroblast cells, whereas they were greatest against normal cells (97.3%). After 48 hours, the 50% inhibitory

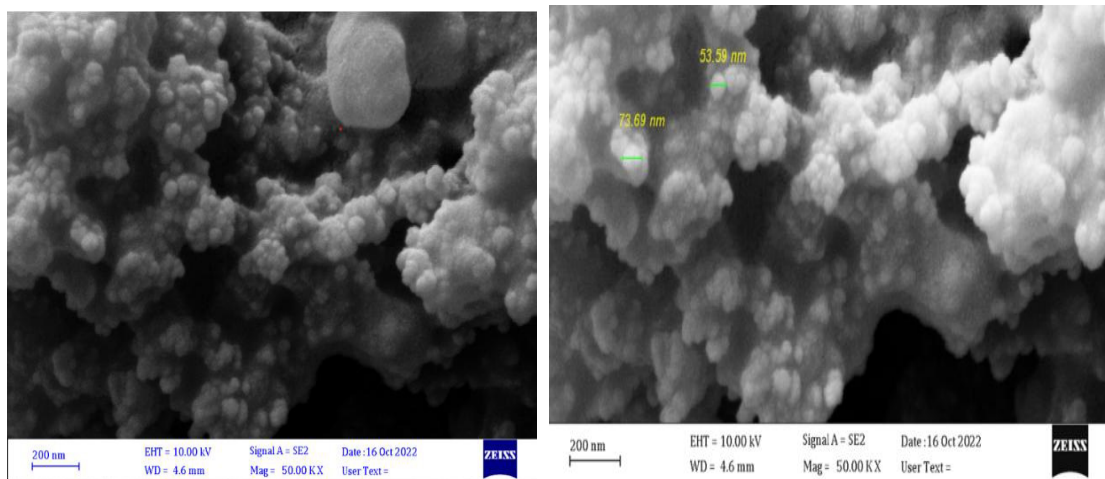


Fig. 5. Histograms of the size distribution of biosynthesized manganese nanoparticles by using milk thistle seeds extract.

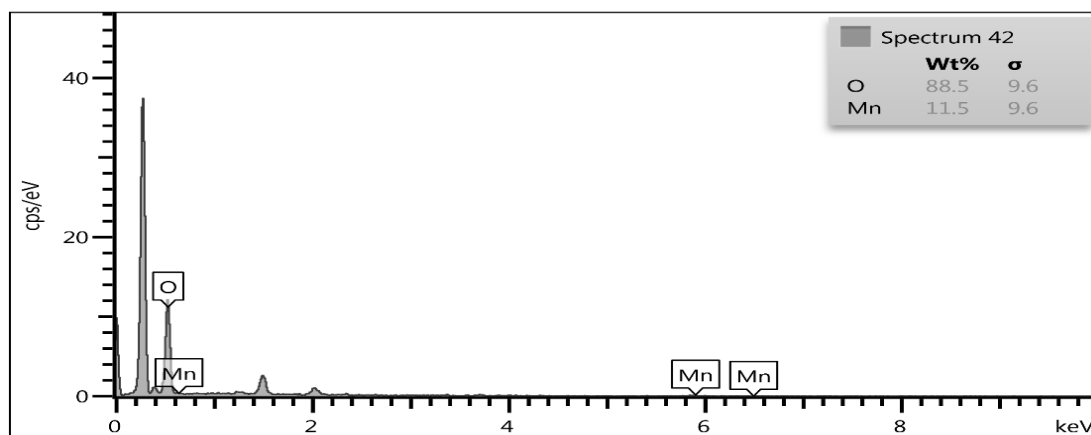


Fig. 6. Energy disperse x-ray analysis spectra of manganese nanoparticles by using milk thistle seed extract.

concentration (IC50) values for this experiment were 24.3 g/ml.

Previous studies that support the present findings pointed to peak adsorption at 420nm for MnO<sub>2</sub> nanoparticles [15].

The spectral data were obtained over a wavenumber interval spanning from 4000 to 450 cm<sup>-1</sup>. The spectrum obtained from Fourier-transform infrared (FT-IR) analysis displays distinguishable peaks that serve as indicators of

chemical functional groups. The data obtained from the experiment indicates the presence of a peak at 3850 and 3797 cm<sup>-1</sup>, which can be associated with the stretching of –OH in either water or ethanol within the system and this finding is like that of Fatma [16] . Nika [17] reported that the O-H group has been assigned to the weak broadband that falls within the range of 2351 and 2316 cm<sup>-1</sup>. The C=O stretching peak, which was observed at 1625 cm<sup>-1</sup>, experienced a redshift to

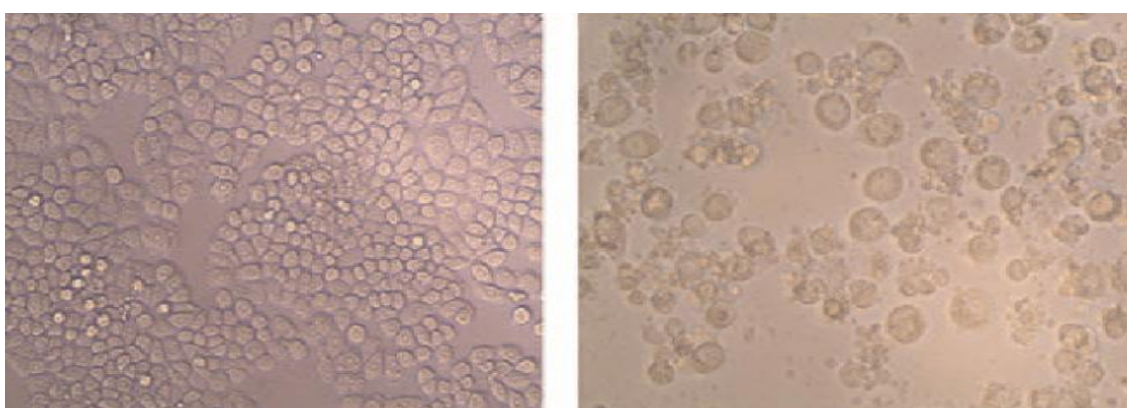


Fig. 7. MDA-MB468 breast cancer cell line: A – untreated, B-treated with manganese nanoparticles using milk thistle seeds extract.

Table 1. Cytotoxicity activity of manganese nanoparticles against MDA MB 468 cells at different concentrations by MTT assay.

Mn NP Conce. µg/ml	Absorbance	Inhibition %	IC 50 µg/ml	p. value
12.5	0.79	- 31		0.67
25	0.63	- 4.3	32.4	0.006*
50	0.37	32.8		0.004*
100	0.69	101.8		0.004*
200	0.043	107.1		0.004*
400	0.041	105.3		0.004*

\*Significant P value <0.05 not significant P value > 0.05

Table 2. Cytotoxicity activity of manganese nanoparticles against normal fibroblast cells at different concentrations by MTT assay.

Mn NP Conce. µg/ml	Absorbance	Inhibition %	IC 50 µg/ml	p. value
12.5	0.183	-31.5		0.054
25	0.258	45.4	24.3	0.166
50	0.112	85.7		0.074
100	0.066	97.3		0.062
200	0.070	95.5		0.065
400	0.082	94.4		0.065

\*Significant P value <0.05 Nonsignificant P value > 0.05

1704  $\text{cm}^{-1}$  due to its interaction with manganese nanoparticles. The spectral data were acquired within the wavenumber range of 4000-450  $\text{cm}^{-1}$ . The Fourier-transform infrared (FT-IR) spectrum exhibits discernible peaks that are indicative of specific chemical functionalities. The obtained data reveals a peak at 3850 and 3797  $\text{cm}^{-1}$ , which can be attributed to the -OH stretching of either water or ethanol present in the system, as reported by [16]. The spectral range of 2351 to 2316  $\text{cm}^{-1}$  has been identified as exhibiting broadband, which has been attributed to the O-H functional group, according to the findings reported by [17]. The observed C=O stretching peak at 1625  $\text{cm}^{-1}$  underwent a redshift to 1704  $\text{cm}^{-1}$ , which can be attributed to the interaction between the C=O group and manganese nanoparticles. Kotval [18] reported that the confirmation of the existence of aromatic unsaturation (C=C) is indicated by the observation of two distinct peaks at 1471 and 1456  $\text{cm}^{-1}$ . The peak of absorption observed at 1397  $\text{cm}^{-1}$  corresponds to the C-N stretch band of the adsorbed water molecules present on the surface of the Mn nanoparticles. The identification of the (C-O) band associated with curcumin was achieved through the observation of peaks at 1197  $\text{cm}^{-1}$  and 1136  $\text{cm}^{-1}$ . A significant absorption signal at 687  $\text{cm}^{-1}$  was identified, corresponding to the typical stretching bonds O-Mn-O, proving the presence of  $\text{MnO}_2$  nanoparticles in the sample [19].

The findings from X-ray diffraction (XRD) analysis confirmed the emergence of manganese oxide, which is consistent with the previous research [20]. Also according to (Narender [21], the manganese oxide's form was found to be roughly crystalline. The identification of certain sounds indicated the existence of impurities that could be attributed to insufficient heating, as reported by [22]. The characterization of microstructure and surface morphology of nanoparticles is commonly achieved through the utilization of X-ray diffraction (XRD) and Field emission electron microscopy (FESEM) techniques. The MnO nanoparticles that were synthesized exhibited a spherical morphology and were devoid of any impurities.

The results of the FESEM analysis indicate that the mean particle size ranged from 52 to 57 nm and exhibited a spherical morphology. According to Prasad and Patra's [23] findings, the manganese oxide nanoparticles produced from the extract of the *Phyllanthus amarus* plant were observed to be spherical in shape and measured between 40-

50 nm. These results are consistent with previous studies on the topic. The progress in the size of MnO nanoparticles is attributed to the process of aggregation and agglomeration, which is a result of their increased number and larger surface area.

Suriyavathana and Ramalingam [15] say that the energy-absorbing band of Mn shown here is correct. So, this proves that the molecules in the plant filtrate were used to make the MnO NPs.

Several findings concluded that the anticancer activity of Mn NP was not returned to cytotoxicity only but to its antioxidant nature [24]. Researchers recently found that Mn NP's anti-proliferative effects on metastatic breast cancer cells (MDA-MB231) were caused by the activation of the standard apoptotic response. This involved an increase in cytochrome c, a reduction in the permeability of the mitochondrial membrane, an increase in caspase activity, and DNA fragmentation [25]. These changes are characteristic of the mitochondrial pathway of the apoptosis pathway [26]. Tang [27] found that Mn-NPs made it more likely that a disturbance of redox balance would lead to tumor cell entering apoptosis and becoming ROS-dependent ferroptosis. Yang [28] did a study that showed that Mn-NPs can kill tumors by working as a system for drug delivery and an agent for oxygenation. Mn-doped silica NPs that contained sorafenib, a special chemotherapy drug for liver cancer, worked well against [29].

After breast cancer cells MDA-MB486 were treated with Mn NP, G1 was stopped. This was because p21 activity went up and CDKs activity went down [30,31].

## CONCLUSION

The green synthesis of manganese nanoparticles (Mn-NPs) utilizing natural extracts presents a promising alternative to conventional chemical synthesis methods. The successful formation of Mn-NPs was confirmed through visual color change, UV spectroscopy, FT-IR, XRD, FE-SEM, and EDX analyses, which collectively validated the structural and morphological characteristics of the synthesized nanoparticles. FE-SEM analysis revealed a spherical shape with a particle size ranging between 52-57 nm, confirming effective nanoparticle formation. Furthermore, cytotoxicity assays demonstrated that Mn-NPs exhibited a dose-dependent inhibitory effect on breast cancer cells (MDA-MB-468), with significant growth inhibition observed at concentrations of

50 µg/ml and above. The highest cytotoxic effect was recorded at 200 µg/ml, showing over 100% cell growth inhibition. Interestingly, the findings also indicated a substantial inhibitory impact on normal fibroblast cells, emphasizing the necessity for further investigations into selective toxicity. Overall, these results highlight the potential of Mn-NPs as a biocompatible anticancer agent. Their dual role in oxidative stress modulation and apoptotic pathway activation suggests that Mn-NPs could serve as a foundation for novel cancer therapies. Future research should aim to optimize selectivity, reduce cytotoxicity in healthy cells, and explore their integration into targeted drug delivery systems.

#### ACKNOWLEDGMENTS

Deep thanks conveyed to the laboratory staff of the Material kits department for all kinds of help and for the Center which they offered me to accomplish this work. Also, the authors are grateful to Al-Bayan University for their enthusiastic assistance and continuous support.

#### CONFLICT OF INTEREST

The authors declare that there is no conflict of interests regarding the publication of this manuscript.

#### REFERENCES

1. Wang EC, Wang AZ. Nanoparticles and their applications in cell and molecular biology. *Integrative biology : quantitative biosciences from nano to macro*. 2014;6(1):9-26.
2. Kai-Hua Chow E, Gu M, Xu J. Carbon nanomaterials: fundamental concepts, biological interactions, and clinical applications. *Nanoparticles for Biomedical Applications*: Elsevier; 2020. p. 223-242. <http://dx.doi.org/10.1016/b978-0-12-816662-8.00014-x>
3. Pandit C, Roy A, Ghotekar S, Khusro A, Islam MN, Emran TB, et al. Biological agents for synthesis of nanoparticles and their applications. *Journal of King Saud University - Science*. 2022;34(3):101869.
4. Zangeneh MM, Bovandi S, Gharehyakheh S, Zangeneh A, Irani P. Green synthesis and chemical characterization of silver nanoparticles obtained using *Allium saralicum* aqueous extract and survey of in vitro antioxidant, cytotoxic, antibacterial and antifungal properties. *Appl Organomet Chem*. 2019;33(7).
5. Martin JD, Cabral H, Stylianopoulos T, Jain RK. Improving cancer immunotherapy using nanomedicines: progress, opportunities and challenges. *Nature reviews Clinical oncology*. 2020;17(4):251-266.
6. Marceddu R, Dinolfo L, Carrubba A, Sarno M, Di Miceli G. Milk Thistle (*Silybum Marianum* L.) as a Novel Multipurpose Crop for Agriculture in Marginal Environments: A Review. *Agronomy*. 2022;12(3):729.
7. Smolarz B, Nowak AZ, Romanowicz H. Breast Cancer-Epidemiology, Classification, Pathogenesis and Treatment (Review of Literature). *Cancers (Basel)*. 2022;14(10):2569.
8. Patra D, El Kurdi R. Curcumin as a novel reducing and stabilizing agent for the green synthesis of metallic nanoparticles. *Green Chemistry Letters and Reviews*. 2021;14(3):474-487.
9. Cailleau R, Olivé M, Cruciger QVJ. Long-term human breast carcinoma cell lines of metastatic origin: Preliminary characterization. *In Vitro*. 1978;14(11):911-915.
10. Ghanbariasad A, Valizadeh A, Ghadimi SN, Fereidouni Z, Osanloo M. Nanoformulating *Cinnamomum zeylanicum* essential oil with an extreme effect on *Leishmania tropica* and *Leishmania major*. *J Drug Deliv Sci Technol*. 2021;63:102436.
11. Adil BH, Al-Shammari AM, Murbat HH. Breast cancer treatment using cold atmospheric plasma generated by the FE-DBD scheme. *Clinical Plasma Medicine*. 2020;19-20:100103.
12. Abdullah SA, Al-Shammari AM, Lateef SA. Attenuated measles vaccine strain have potent oncolytic activity against Iraqi patient derived breast cancer cell line. *Saudi J Biol Sci*. 2020;27(3):865-872.
13. Al-Shammari AM, Jalill RDA, Hussein MF. Combined therapy of oncolytic Newcastle disease virus and rhizomes extract of *Rheum ribes* enhances cancer virotherapy in vitro and in vivo. *Mol Biol Rep*. 2020;47(3):1691-1702.
14. Al-Shammari AM, Rameez H, Al-Tae MF. Newcastle disease virus, rituximab, and doxorubicin combination as anti-hematological malignancy therapy. *Oncolytic virotherapy*. 2016;5:27-34.
15. Rakkimuthu R, Aarthi S, Neelamathi E, Sathishkumar P, Anandakumar AM, Sowmiya D. Green Synthesis of Reduced Graphene Oxide Silver Nanocomposite Using *Anisomeles malabarica* (L.) R. BR. LEAF EXTRACT AND ITS

- ANTIBACTERIAL ACTIVITY. *Rasayan Journal of Chemistry*. 2022;15(01):417-422.
16. Renganathan S, Fatma S, P K. Green Synthesis of Copper Nanoparticle from *Passiflora Foetida* Leaf Extract and Its Antibacterial Activity. *Asian Journal of Pharmaceutical and Clinical Research*. 2017;10(4):79.
  17. Naika HR, Lingaraju K, Manjunath K, Kumar D, Nagaraju G, Suresh D, et al. Green synthesis of CuO nanoparticles using *Gloriosa superba* L. extract and their antibacterial activity. *Journal of Taibah University for Science*. 2015;9(1):7-12.
  18. Kotval SC, John T, Parmar KA. Green Synthesis of Copper Nanoparticles using *Mitragyna parvifolia* Plant Bark Extract and Its Antimicrobial Study. *Journal of Nanoscience and Technology*. 2018;4(4):456-460.
  19. Estelrich J, Sánchez-Martín MJ, Busquets MA. Nanoparticles in magnetic resonance imaging: from simple to dual contrast agents. *International journal of nanomedicine*. 2015;10:1727-1741.
  20. Investigations on Synthesis, Structural, Morphological and Dielectric Properties of Manganese Oxides Nanoparticles. *Journal of Material Science & Engineering*. 2015;04(03).
  21. Narender SS, Varma VVS, Srikar CS, Ruchitha J, Varma PA, Praveen BVS. Nickel Oxide Nanoparticles: A Brief Review of Their Synthesis, Characterization, and Applications. *Chemical Engineering and Technology*. 2022;45(3):397-409.
  22. Kolya H, Maiti P, Pandey A, Tripathy T. Green synthesis of silver nanoparticles with antimicrobial and azo dye (Congo red) degradation properties using *Amaranthus gangeticus* Linn leaf extract. *Journal of Analytical Science and Technology*. 2015;6(1).
  23. Prasad KS, Patra A. Green synthesis of MnO<sub>2</sub> nanorods using *Phyllanthus amarus* plant extract and their fluorescence studies. *nano Online: De Gruyter*; 2018. <http://dx.doi.org/10.1515/nano.0015.00032>
  24. Li L, Yang X. The Essential Element Manganese, Oxidative Stress, and Metabolic Diseases: Links and Interactions. *Oxid Med Cell Longev*. 2018;2018:7580707-7580707.
  25. Jiang K, Wang W, Jin X, Wang Z, Ji Z, Meng G. Silibinin, a natural flavonoid, induces autophagy via ROS-dependent mitochondrial dysfunction and loss of ATP involving BNIP3 in human MCF7 breast cancer cells. *Oncol Rep*. 2015;33(6):2711-2718.
  26. Anderson NM, Simon MC. The tumor microenvironment. *Current biology : CB*. 2020;30(16):R921-R925.
  27. Tang H, Li C, Zhang Y, Zheng H, Cheng Y, Zhu J, et al. Targeted Manganese doped silica nano GSH-cleaner for treatment of Liver Cancer by destroying the intracellular redox homeostasis. *Theranostics*. 2020;10(21):9865-9887.
  28. Yang M, Li J, Gu P, Fan X. The application of nanoparticles in cancer immunotherapy: Targeting tumor microenvironment. *Bioactive materials*. 2020;6(7):1973-1987.
  29. Atif M, Iqbal S, Fakhar-E-Alam M, Ismail M, Mansoor Q, Mughal L, et al. Manganese-Doped Cerium Oxide Nanocomposite Induced Photodynamic Therapy in MCF-7 Cancer Cells and Antibacterial Activity. *BioMed research international*. 2019;2019:7156828-7156828.
  30. Erratum: Cytotoxicity and physicochemical characterization of iron-manganese-doped sulfated zirconia nanoparticles [Corrigendum]. *International journal of nanomedicine*. 2015;10:6657-6657.
  31. Pirouzpanah MB, Sabzichi M, Pirouzpanah S, Chavoshi H, Samadi N. Silibinin-Induces Apoptosis in Breast Cancer Cells by Modulating p53, p21, Bak and Bcl-xl Pathways. *Asian Pac J Cancer Prev*. 2015;16(5):2087-2092.